Dispersion Engineering with Photonic Inverse Design

Dries Vercruysse, Neil V. Sapra, Logan Su, and Jelena Vučković *Fellow, IEEE*

(Invited Paper)

***Abstract*—Dispersion engineering, such as design of slow light waveguide systems, is an effective tool for a wide range of photonic applications, but present a difficult optical design challenge. Most applications require a slow light waveguide design that mitigates group velocity dispersion, and efficient coupling solutions over the slow light operating bandwidth. In this work, we optimize the slow-light dispersion relation of a photonic crystal waveguide with three dimensional (3D) inverse design methods. In addition, we design mode couplers to the photonic crystal waveguide. The optimized waveguide supports a slow light mode with a group index of $\mathbf{n_g = 25}$ and a normalized bandwidth group index product of $\mathbf{0.38}$. A compact mode coupler to a strip waveguide is designed with an average efficiency of $\mathbf{92.7\%}$ within the slow light operating bandwidth. Lastly, we design a full etch grating which couples directly to the slow light mode with a $\mathbf{32.5\%}$ average efficiency.**

***Index Terms*—inverse design, slow light, dispersion engineering, phase delay, photonic crystal waveguide, mode converter, grating coupler.**

I. Introduction

SLOW light photonic crystal waveguides play a pivotal role in exploring and enhancing photonic processes at the chip level. The low group velocity enables strong light-matter interactions and facilitates new device functionalities. Slow light (SL) waveguides have been used to enhance nonlinear effects, two-photon absorption, and interaction with gain material or quantum systems [1]–[5]. Furthermore, the low-slope dispersion relation, which characterizes slow light, results in a large phase velocity change for a wavelength shift or a change in the waveguide's refractive index. This has made SL waveguides a powerful basis for optical switching, as well as for optical sensing [6]–[9].

Early SL photonic crystal waveguide devices relied on a simple line-defect in hexagonal lattice. These devices suffers from a large group velocity dispersion, as well as high losses. Remedying these drawbacks gave rise to the field of dispersion engineering, where alteration of the photonic crystal waveguide periodic structure, e.g. resizing or shifting holes, tailors the photonic crystal waveguide properties for the intended application [10], [11]. Furthermore, mode mismatch between the SL waveguide and a strip waveguide, commonly used for on-chip routing, can lead to large insertion losses. Tapering has shown high coupling efficiencies up to 97% for non-dispersion engineered photonic crystal waveguides. [12] However, optimizing the transitions to an altered photonic crystal waveguide has proven to be more difficult [13]. Considerable efforts have therefore been aimed at improving the coupling efficiency to dispersion engineered waveguides [10], [14]. Classical design methods for photonic crystal waveguides and couplers still rely on a trial-and-error approach, forming a barrier for their use in applications.

The advent of photonic inverse design has resulted in considerable improvements in the design of integrated photonics [15]–[19]. Moving away from simple parameter sweeps, optimizing arbitrary topologies has allowed for increased device efficiencies and novel functionalities. Early on, inverse design was recognized as a powerful tool for designing photonic crystals, generating new band gaps lattices and shaping band edges [20]–[24]. Similarly, inverse design was shown to be capable to improve the group velocity dispersion of SL waveguides, as well as full pulse delay devices [25], [26].

In this work, we use the inverse design methods to design a SL waveguide, as well as coupling solutions to this SL waveguide from a strip waveguide and from free-space. Unlike most related work on photonic crystal waveguide optimization, we rely on full 3D simulations instead of 2D simulations. 2D simulations, while computationally efficient, often do not provide a representative optimization topology, do not capture losses of 3D devices and do not allow for designs with out-of-plane optical interactions. Considering the computational cost of the 3D simulation we do not optimize the slow light system as a whole, as was done in 2D [26]. Rather, we optimize the components of the system separately. We first present the optimization problems for both the SL photonic crystal waveguide and the couplers. Subsequently, the different optimized components (the waveguide, mode converter and grating coupler) are optimized through the inverse design method, and the resulting designs and performance are presented.

II. Inverse design optimization problems

Inverse design problems for optical devices are of the form:

$$\begin{aligned} \underset{p,E_1,\ldots,E_n}{\text{minimize}} \quad & f_{obj}(p, E_1, \ldots E_n) + \alpha\ g_{fab}(p) \\ \text{subject to} \quad & h_{EMi}(p, E_i) = 0,\ i = 1, \ldots, n, \end{aligned} \tag{1}$$

The objective function, f_{obj}, defines a figure of merit, which need to be minimized as a function of a parametrization vector, p, which describes the device structure, and the optical fields, E_i, for a number of different modes i, e.g. different wavelengths. The optical fields are linked to the structure by constraining the problem to Maxwell's equations, h_{EM}. Furthermore, to ensure the fabricability of the device, we can add a penalty function, g_{fab}, to the objective with a weight

All authors are with the Ginzton Laboratory, Stanford University, Stanford, California 94305, USA

Manuscript received June 14, 2019; revised XXX XX, 2019.

factor, α. In this work we use the penalty function described in [27], which penalizes gaps and curvature in the design.

A. Slow light waveguide

Slow light waveguide design aims to obtain a periodic structure with a low-slope linear dispersion relation, within a certain bandwidth. Different figures-of-merits can be devised for the optimization of these waveguides. The most direct way would be to minimize the absolute difference between the group velocity of the structure and the desired group velocity for in a series of wavevectors, k_i [28]. While effective, this method is computationally expensive and prohibitive for optimization with full 3D simulations, since the derivative of the group velocity requires an additional adjoint simulation. Alternatively, for a series of wavevectors, we can optimize the difference between the different frequencies [25]. Here, the derivative of the frequencies can be constructed with the eigenvectors and thus does not require an additional solve (Suppl. Info.). In this case the objective function becomes:

$$f_{obj}(p) = \mathcal{F}\big(\{(\omega_{i+1}(p) - \omega_i(p) - \Delta\omega_i)^2 | i = 1, \ldots, n-1\}\big) \tag{2}$$

where ω_i is the angular frequency associate with k_i and $\Delta\omega_i$ is the target frequency difference. In order to reach a certain target group index, n_g, $\Delta\omega_i$ is set to $\frac{k_{i+1}-k_i}{n_g}$. $\mathcal{F}$ is a function that combines and weighs the elements of set, and can be implemented as a sum, the maximum, or the softmax function.

The underlying physics constraint, h_{EM}, for this optimization problem describes the dispersion relation, which results from the eigenvalue problem:

$$h_{EM\,i} = \nabla_k \times \frac{1}{\mu}\nabla_k \times E_i - \omega_i^2 \epsilon(p) E_i = 0, \tag{3}$$

where $\mu = 1$ is the permeability, and $\epsilon(p)$ is the permittivity of the structure, parametrized by p. $\nabla_k \times$ is the curl-operator taking the bloch boundary condition for wavevector, $\vec{k}$, into account.

B. Slow light waveguide coupler

Coupling light to the SL mode can be challenging due to low modal overlap and the large group index mismatch. This leads to strong reflections and large insertion loss. Most slow light photonic systems therefore incorporate tapers or mode coupling devices. For a SL waveguide coupler, we need to optimize the transmission in the waveguide mode. Considering the input power of the source is normalized to unity, the objective then becomes:

$$f_{obj}(E_1, \ldots, E_n) = \sum_{i=1}^{n} 1 - |C_i \cdot E_i|^2 \tag{4}$$

where C_i is a vector which evaluated the modal overlap for the waveguide mode in a specific propagation direction. [29].

The electromagnetic constraint for this problem becomes:

$$h_{EM\,i} = \nabla \times \frac{1}{\mu}\nabla \times E_i - \omega_i^2 \epsilon(p) E_i + j\omega_i J_i = 0 \tag{5}$$

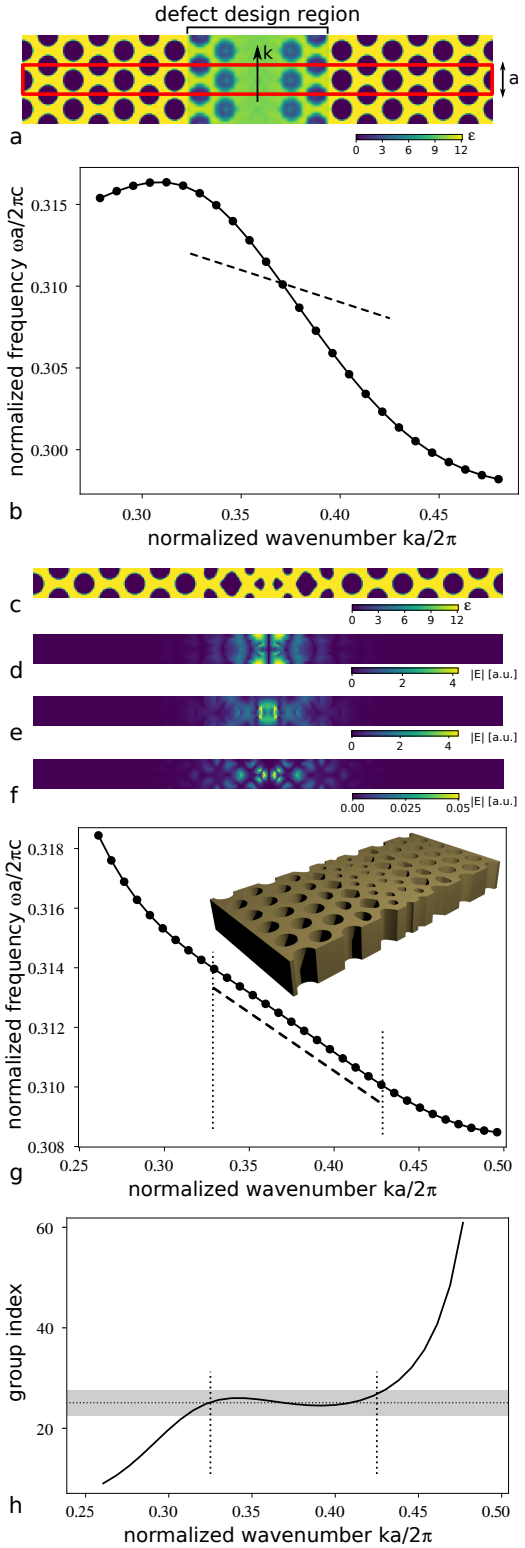

Fig. 1. Slow light photonic crystal waveguide optimization. (a) Initial permittivity distribution. The red box indicates the waveguide unit cell with lattice constant, a. (b) Initial dispersion relation. The dashed line indicates the target dispersion slope. (c) Final optimized permittivity distribution. (d,e,f) Electric field magnitude, E_x, E_y and E_z, respectively (g) Final dispersion relation and (h) final group index. The dashed line in (g) indicates the target dispersion slope. The gray area shows the $\pm 10\%$ group index error. The dotted lines in (g) and (h) indicate the wavenumber interval used in the optimization.

Here the fields, E_i, result from the sources, J_i, corresonding either the input waveguide mode or a vertically incident gaussian beam, in case of waveguide coupler or grating coupler, respectively.

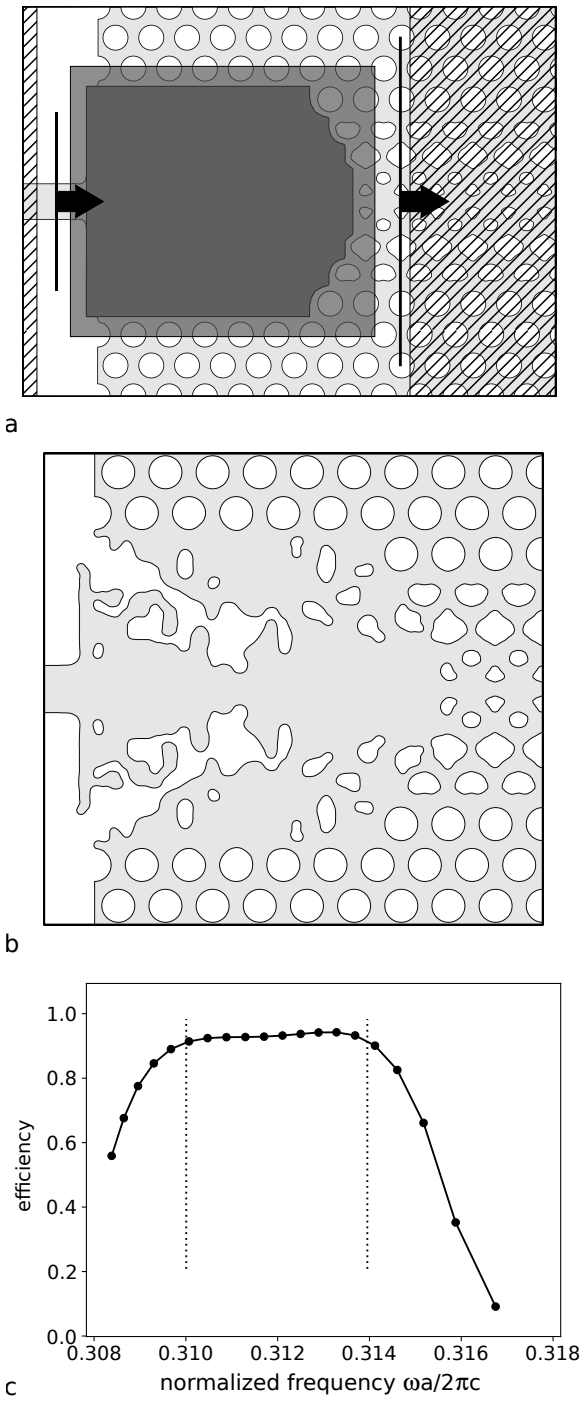

Fig. 2. Strip waveguide to SL photonic crystal waveguide coupler. (a) Simulation set-up. The hatched area indicate PML regions. The shaded and dark region indicate the design regions. The vertical lines with arrows on the left and right of the design area indicate the source and modal overlap, respectively. (b) Final structure. (c) Mode conversion efficiency of the final structures. The dotted lines mark the slow light operation interval.

III. Slow light waveguide

The SL waveguide is based on an air-suspended silicon ($\epsilon = 12.11$) slab with a hexagonal lattice with a lattice constant $a = 400nm$. The radius of the holes are $0.35a$ and the thickness of the slab is $0.55a$. The optimization starts from a single line-defect PhC waveguide of which both sides are shifted apart by an additional $0.26a$. The design region of the waveguide is $4.74a$ wide, encompassing row 1 and 2 on the side of the defect line. The structure is mapped onto a uniform Yee-grid with a $a/20$ pitch [30]. In order to avoid very small features, we do not parametrize the design region on this grid directly but use a coarse control grid with a $a/6$ pitch. The permittivity of the simulation grid is the result of a cubic interpolation of these coarse grid parametrization values [27]. Furthermore, in this problem, we do not use a fabrication penalty.

The optimization starts with a continuous parametrization, i.e the permittivity in the design region can take any value in between that of silicon and air. The initial condition is derived from the $W^{1.26}$ line-defect [12]. Outside the defect design region, the regular hexagonal lattice is drawn. Inside the design region, the continuous parametrization has been fitted to the line-defect and smoothed, resulting in the unit cell shown in Figure 1a. The continuous parametrization allows for more aggressive changes to the structure, e.g., forming new holes, compared to the levelset parametrization used later on in the optimization process. Starting with this continuous relaxation typically results in better starting conditions for the levelset optimization.

The dispersion relation of this initial PhC waveguide is shown in Figure 1b. The optimization objective using this continuous optimization is Eq. (2) and uses eight wavenumbers spanning from $0.325\frac{2\pi}{a}$ to $0.425\frac{2\pi}{a}$. The $\Delta\omega$ is chosen to have a group index of 25, so that the photonic crystal waveguide has a bandwidth of roughly $20nm$ around $1300nm$. The weight function used in Eq. (2) is a simple sum.

After 45 iterations of optimization using limited-memory Broyden-Fletcher-Goldfarb-Shanno (L-BFGS) as optimization method and the continuous permittivity parametrization, we transition to a levelset parametrization [31]. A levelset parametrization is a continuous function which defines waveguide material where it is positive and air where it is negative. This parametrization thus describes an arbitrary binary structure which can be fabricated. After fitting the levelset parametrization the permittivity distribution described by the continuous parametrization, we optimize with L-BFGS for an additional 25 iterations using the same objective function as before, and conclude with 24 iterations using Eq. (2) as the objective function, but with softmax as the weight function.

The final optimized structure as well as the fields for $k = 0.375\frac{2\pi}{a}$ can be seen in Figure 1c-f. The band diagram of this structure is shown in Figure 1g. In between the $[0.325\frac{2\pi}{a}, 0.425\frac{2\pi}{a}]$ wavenumber interval we reach an average group index of 25.14, which is close to the $n_g = 25$ target value. Considering the group index is typically evaluated with a 10% margin of error, the wavenumber interval can be extended to $[0.31\frac{2\pi}{a}, 0.43\frac{2\pi}{a}]$ around $\omega = 0.312\frac{2\pi c}{a}$, resulting in a normalized bandwidth group index product, NBGP, of

0.38 [32].

IV. Slow light to strip waveguide coupler

A mode converter for the SL waveguide of Figure 1c was designed with inverse design using the objective function of Eq. (4). We use four modes corresponding to the frequencies for $k = [0.330, 0.360, 0.390, 0.420]\frac{2\pi}{a}$. The simulation set-up for this problem is depicted in Figure 2a. The strip waveguide mode is injected from the left towards the design region by a total-field-scattered-field (TFSF) source. On the right of the design region the modal overlap with the slow light mode in the photonic crystal waveguide is evaluated. To reduce reflections of the slow light mode with the Stretched-Coordinate Perfectly-Matched Layer (SC-PML) boundary condition, we use 80 layers, as apposed to 10 layers, which is typically used [33]. The inner design region (dark gray) is used in the first optimization stage where the parametrization allows for continuous permittivity values. The region is adapted so as not to cut though any photonic crystal holes. We leave $60nm$ distance between design area and the holes. The final optimization, which uses a level-set optimization, modifies the outer design region (semi-transparent gray). During this stage the PhC holes that overlap with this design area can be altered. Finally, in addition to the EM constraint, a fabrication penalty for a feature size of $50nm$ is added to the optimization objective.

The optimization consisted of 45 L-BFGS iteration with continuous parametrization, followed by 52 L-BFGS iterations with level-set parametrization. The resulting structure contained unconnected features. As the structure is suspended, i.e. air cladding above and below, these unconnected features are not allowed. We therefore manually connected these features to the main structure and re-optimized. The final fully connected design can be seen in Figure 2b, and the coupling efficiency is shown in Figure 2c. Within the slow light frequency interval (dashed lines), the device achieves an average coupling efficiency of 92.7%.

V. Slow light grating coupler

Light from a fiber or free space is commonly coupled on to a chip by using end-coupling or grating couplers; however, grating couplers are often prefered due to ease of alignment. A grating coupler is typically followed by a waveguide taper with a considerable length in order to transition to a single mode waveguide. Here, we aim to design a grating coupler which couples directly into the slow light waveguide from a focused beam.

The simulation set-up for this optimization can be seen in Figure 2a. The source depicted in the top inset is a TFSF Gaussian beam source with a beam waist radius of $1\mu m$ positioned $400nm$ above the waveguide slab. The design area is $3.7 \times 3.7\mu m$. For the objective function we again rely in Eq. 4, which evaluates the modal overlap with slow light PhC mode on the left side of the design area. As with the strip waveguide coupler, we add a fabrication penalty for $50nm$ to the objective.

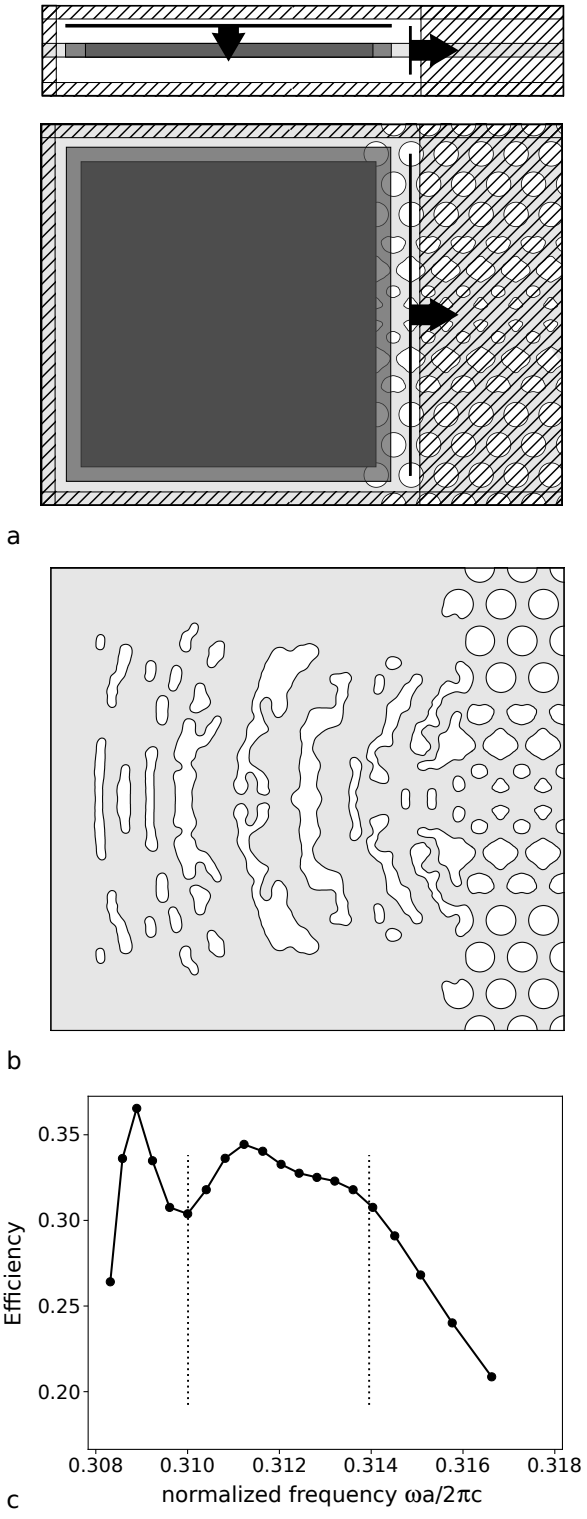

Fig. 3. Free-space to slow light photonic crystal waveguide grating coupler. (a) Side (top) and top (bottom) view of the simulation set-up. The hatched area indicate PML regions, the shaded and dark region indicate the design regions. (b) Final structure from optimization. (c) Grating coupling efficiency of the final structure. The dotted lines mark the slow light frequency interval.

The final structure is shown in Figure 3b. The optimization consists of 30 L-BFGS iterations with a contin-

uous parametrization and 62 L-BFGS iterations with level-set parametrization. The coupling efficiency of the optimized structure is shown in Figure 3b. Similarly as for the strip waveguide coupler, the efficiency is high within the optimization window and decreased strongly for higher frequencies. Within the slow light frequency interval, the structure reaches a 32.5% average efficiency. Since a full etch is used here, the structure is symmetric in the z-axis, making the maximum achievable efficiency for the device 50%. The efficiency could be improved further by using a Gaussian beam with an angled incidence, breaking the vertical symmetry (e.g., using a partial or slanted etch), or placing a reflector under the structure.

VI. Conclusion

In this work, we optimize different components of an integrated slow light waveguide system using inverse design methods. A photonic crystal waveguide was optimized for a particular group index value with minimal group velocity dispersion. The resulting waveguide has a NBGP of 0.38. Subsequently, we optimized couplers for this SL waveguide: a strip waveguide mode converter with an 92.7% average efficiency, and a full etch grating coupler with an average efficiency of 32.5%. All optimizations were carried out using full-3D solvers. The computational cost of optimizing the slow light photonic system stayed manageable by separating the slow light waveguide systems in waveguide and coupling problems. This demonstration of implementable designs for slow light systems heralds the use of inverse design for larger integrated photonic systems which can benefit form slow light waveguides, such as modulators, filters or phased arrays.

Acknowledgment

D.V. acknowledges funding from FWO and European Union's Horizon 2020 research and innovation program under the Marie Sklodowska-Curie grant agreement No 665501. N.V.S. and J.V. acknowledge funding from the Gordon and Betty Moore Foundation (GBMF4744). L.S. and J.V. acknowledge funding from Google. We acknowledge support from the ERFI NewLaw program under the NSF award number 1741660. We also thank Google for providing computational resources on the Google Cloud Platform.

References

[1] B. Corcoran, C. Monat, C. Grillet, D. J. Moss, B. J. Eggleton, T. P. White, L. O'Faolain, and T. F. Krauss. Green light emission in silicon through slow-light enhanced third-harmonic generation in photonic-crystal waveguides. *Nature Photonics*, 3(4):206–210, 2009.

[2] C. Monat, B. Corcoran, C. Grillet, M. Ebnali-Heidari, D. J. Moss, B. J. Eggleton, T. P. White, L. O'Faolain, and T. F. Krauss. Slow Light Enhanced Nonlinear Effects in Silicon Photonic Crystal Waveguides. 17(4):JWB1, 2013.

[3] Ryo Hayakawa, Norihiro Ishikura, Hong C. Nguyen, and Toshihiko Baba. Two-photon-absorption photodiodes in Si photonic-crystal slow-light waveguides. *Applied Physics Letters*, 102(3):1–4, 2013.

[4] Sara Ek, Per Lunnemann, Yaohui Chen, Elizaveta Semenova, Kresten Yvind, and Jesper Mork. Slow-light-enhanced gain in active photonic crystal waveguides. *Nature Communications*, 5:1–7, 2014.

[5] J. S. Douglas, H. Habibian, C. L. Hung, A. V. Gorshkov, H. J. Kimble, and D. E. Chang. Quantum many-body models with cold atoms coupled to photonic crystals. *Nature Photonics*, 9(5):326–331, 2015.

[6] Yosuke Terada, Keisuke Kondo, Ryotaro Abe, and Toshihiko Baba. Full C-band Si photonic crystal waveguide modulator. *Optics Letters*, 42(24):5110, 2017.

[7] Toshihiko Baba, Hong C. Nguyen, Naoya Yazawa, Yosuke Terada, Satoshi Hashimoto, and Tomohiko Watanabe. Slow-light Mach-Zehnder modulators based on Si photonic crystals, 2014.

[8] Amit Kumar Goyal and Suchandan Pal. Design and simulation of high sensitive photonic crystal waveguide sensor. *Optik*, 126(2):240–243, 2015.

[9] Hai Yan, Chun Ju Yang, Naimei Tang, Yi Zou, Swapnajit Chakravarty, Amanda Roth, and Ray T. Chen. Specific Detection of Antibiotics by Silicon-on-Chip Photonic Crystal Biosensor Arrays. *IEEE Sensors Journal*, 17(18):5915–5919, 2017.

[10] Yong Zhao, Ya-Nan Zhang, Qi Wang, and Haifeng Hu. Review on the Optimization Methods of Slow Light in Photonic Crystal Waveguide. *IEEE transactions on nanotechnology*, 14(3):407–426, 2015.

[11] Sebastian A. Schulz, Jeremy Upham, Liam O'Faolain, and Robert W. Boyd. Photonic crystal slow light waveguides in a kagome lattice. *Optics Letters*, 42(16):3243, 2017.

[12] Pierre Pottier, Marco Gnan, and Richard M. De La Rue. Photonic crystal tapers for coupling into slow-light photonic crystal channel waveguides. *Optics Express*, 15(11):6569–6575, 2007.

[13] Somayyeh Rahimi, Amir Hosseini, Xiaochuan Xu, Harish Subbaraman, and Ray T. Chen. Group-index independent coupling to band engineered SOI photonic crystal waveguide with large slow-down factor. *Optics Express*, 19(22):21832, 2011.

[14] Hemant Sankar Dutta, Amit Kumar Goyal, Varun Srivastava, and Suchandan Pal. Coupling light in photonic crystal waveguides: A review. *Photonics and Nanostructures - Fundamentals and Applications*, 20:41–58, 2016.

[15] Logan Su, Rahul Trivedi, Neil Sapra, Alexander Y. Piggott, Dries Vercruysse, and Jelena Vučković. Fully-automated optimization of grating couplers. *Optics Express*, 26(4):4023–4034, 2018.

[16] Alexander Y. Piggott, Jesse Lu, Konstantinos G. Lagoudakis, Jan Petykiewicz, Thomas M. Babinec, and Jelena Vucković. Inverse design and demonstration of a compact and broadband on-chip wavelength demultiplexer. *Nature Photonics*, 9(6):374–377, 2015.

[17] Logan Su, Alexander Y. Piggott, Neil V. Sapra, Jan Petykiewicz, and Jelena Vučković. Inverse Design and Demonstration of a Compact on-Chip Narrowband Three-Channel Wavelength Demultiplexer. *ACS Photonics*, 5(2):301–305, 2018.

[18] N. V. Sapra, D. Vercruysse, L. Su, K. Y. Yang, J. Skarda, A. Y. Piggott, and J. Vukovi. Inverse design and demonstration of broadband grating couplers. *IEEE Journal of Selected Topics in Quantum Electronics*, 25(3):1–7, May 2019.

[19] Sean Molesky, Zin Lin, Alexander Y. Piggott, Weiliang Jin, Jelena Vuckovic, and Alejandro W. Rodriguez. Outlook for inverse design in nanophotonics. *Nature Photonics*, 12(November), 2018.

[20] Martin Burger, SJ Osher, and Eli Yablonovitch. Inverse problem techniques for the design of photonic crystals. *IEICE transactions on Electronics*, E87-C(3):258–265, 2004.

[21] Chiu Y. Kao, Stanley Osher, and Eli Yablonovitch. Maximizing band gaps in two-dimensional photonic crystals by using level set methods. *Applied Physics B: Lasers and Optics*, 81(2-3):235–244, 2005.

[22] Han Men, Karen Y. K. Lee, Robert M. Freund, Jaime Peraire, and Steven G. Johnson. Robust topology optimization of three-dimensional photonic-crystal band-gap structures. 22(19):263–275, 2014.

[23] Stefan Preble, Michal Lipson, and Hod Lipson. Two-dimensional photonic crystals designed by evolutionary algorithms. *Applied Physics Letters*, 86(6):1–3, 2005.

[24] Joel Goh, Ilya Fushman, Dirk Englund, and Jelena Vuckovic. Genetic Optimization of Photonic Bandgap Structures. 15(13):8218–8230, 2007.

[25] Fengwen Wang, Jakob S. Jensen, and Ole Sigmund. Robust topology optimization of photonic crystal waveguides with tailored dispersion properties. *Journal of the Optical Society of America B*, 28(3):387–397, 2011.

[26] René Matzen, Jakob S. Jensen, and Ole Sigmund. Systematic design of slow-light photonic waveguides. *Journal of the Optical Society of America B*, 28(10):2374, 2011.

[27] Dries Vercruysse, Neil V. Sapra, Logan Su, Rahul Trivedi, and Jelena Vučković. Analytical level set fabrication constraints for inverse design. *Scientific Reports*, 9(1):1–7, 2019.

[28] Fengwen Wang, Jakob S. Jensen, and Ole Sigmund. High-performance slow light photonic crystal waveguides with topology optimized or circular-hole based material layouts. *Photonics and Nanostructures - Fundamentals and Applications*, 10(4):378–388, 2012.

[29] Paul R. McIsaac. Mode Orthogonality in Reciprocal and Nonreciprocal Waveguides. *IEEE Transactions on Microwave Theory and Techniques*, 39(11):1808–1816, 1991.
[30] Kane S. Yee. Yee: Solution of Initial Boundary Value Problems. *Ieee Transaction on Antennas and Propagation*, AP-14(3):302, 1966.
[31] Richard H. Byrd, Peihuang Lu, Jorge Nocedal, and Ciyou Zhu. A limited memory algorithm for bound constrained optimization. *Journal of Scientific Computing*, 16(5):1190–1208, 1995.
[32] Yi Zhai, Huiping Tian, and Yuefeng Ji. Slow light property improvement and optical buffer capability in ring-shape-hole photonic crystal waveguide. *J. Lightwave Technol.*, 29(20):3083–3090, Oct 2011.
[33] Weng Cho Chew and William H. Weedon. A 3D perfectly matched medium from modified maxwell's equations with stretched coordinates. *Microwave and Optical Technology Letters*, 7(13):599–604, 1994.

Dries Vercruysse Dries Vercruysse received the B.S. and M.S. degrees in engineering and Ph.D. in physics from the KU Leuven, Leuven, Belgium, in 2007, 2009, and 2015 respectively. After his Ph.D. he joined IMEC, Leuven, Belgium, as a researcher. In 2016, he received a FWO Pegasus Marie Curie Fellowships for post-doctoral research at Stanford University.

Neil V. Sapra is a doctoral candidate in the Department of Physics at Stanford University. He received his B.S. in computational physics and theoretical computer science from U.C. San Diego in 2015.

His research focuses on developing laser coupling strategies for dielectric laser accelerators and demonstrating waveguide-integrated approaches to these accelerators. Both of these aims rely heavily on inverse design methodologies.

Logan Su is a doctoral candidate in the Department of Applied Physics at Stanford University. He received his B.S.E in Electrical Engineering and Physics from Duke University in 2015.

Jelena Vučković is a Professor of Electrical Engineering and by courtesy of Applied Physics at Stanford, where she leads the Nanoscale and Quantum Photonics Lab. She is also a faculty member of the Ginzton Lab, PULSE Institute, Simes Institute, and Bio-X at Stanford. Upon receiving her PhD degree in Electrical Engineering from the California Institute of Technology (Caltech) in 2002, she worked as a postdoctoral scholar at Stanford. In 2003, she joined the Stanford Electrical Engineering Faculty, first as an assistant professor (until 2008), then an associate professor with tenure (2008-2013), and finally as a professor of electrical engineering (since 2013). As a Humboldt Prize recipient, she has also held a visiting position at the Institute for Physics of the Humboldt University in Berlin, Germany (since 2011). In 2013, she was appointed as a Hans Fischer Senior Fellow at the Institute for Advanced Studies of the Technical University in Munich, Germany.

In addition to the Humboldt Prize (2010) and the Hans Fischer Senior Fellowship (2013), Vučković has received many awards including the Marko V. Jaric award for outstanding achievements in physics (2012), the DARPA Young Faculty Award (2008), the Chambers Faculty Scholarship at Stanford (2008), the Presidential Early Career Award for Scientists and Engineers (PECASE in 2007), the Office of Naval Research Young Investigator Award (2006), the Okawa Foundation Research Grant (2006), and the Frederic E. Terman Fellowship at Stanford (2003). She is a Fellow of the American Physical Society (APS) and of the Optical Society of America (OSA). Vučković is a member of the scientific advisory board of the Max Planck Institute for Quantum Optics - MPQ (in Munich, Germany) and of the scientific advisory board of the Ferdinand Braun Institute (in Berlin, Germany). She is also an Associate Editor of ACS Photonics, a member of the editorial advisory board of Nature Quantum Information, and was on the editorial board of the New Journal of Physics.